

Experimental Investigation of Damage Detection in Composite Material Structures using a Laser Vibrometer and Piezoelectric Actuators

A. GHOSHAL,^{1,*} A. CHATTOPADHYAY,¹ M. J. SCHULZ,² R. THORNBURGH¹ AND K. WALDRON³

¹*Department of Mechanical and Aerospace Engineering, Arizona State University, Tempe, AZ 85287-6106, USA*

²*Department of Mechanical Engineering, University of Cincinnati, Cincinnati, OH 45221-0072, USA*

³*Siemens Westinghouse Power Corporation, Orlando, FL 32826-2399, USA*

ABSTRACT: An experimental investigation to detect embedded delamination and other forms of damage in heterogeneous structures using smart materials and a laser vibrometer is presented. Typically, piezoelectric actuators and sensors have been used for characterizing the presence of damage in composite structures. However, the interpretation of vibration responses in identifying damage using such a procedure is strongly dependent upon the numbers and types of sensors and actuators used. The use of Vibration Deflection Shapes (VDSs), which are the actual vibration patterns of a structure undergoing steady-state vibration, is an alternative approach that is investigated in this paper. Experiments are conducted on composite structures with piezoelectric actuator patches and embedded delaminations, using the VDS method and a Scanning Laser Doppler Vibrometer. The laser vibrometer provides a dense pattern of measurements of the structural response, which effectively increases sensor density compared to the widely spaced piezoceramic sensors used in other techniques. A series of experiments is performed on composite plate-beams with various sizes, ply-level locations, and placement of delaminations to comprehensively evaluate the performance of the laser technique. The VDSs are shown to be sensitive to structural parameter variations, and hence can be used to detect and locate damage in large composite structures, including a woven fiberglass curved plate and a honeycomb intertank panel. The successful experimental demonstration of the procedure using different test articles shows that the VDS method can become an effective and time saving tool for structural health monitoring, particularly for detection of damage in composites.

Key Words: structural health monitoring, composite structures, delamination, laser vibrometry, and vibration deflection shapes

INTRODUCTION

DAMAGE detection can increase safety, extend serviceability, reduce maintenance costs and extend the operating limits of structures. In the case of composite structures, typical damage may include surface cracks, interfacial cracks, delamination, corrosion, propagating fatigue cracks, and distributed fatigue. Among these, embedded damage such as delamination, underlying corrosion, and distributed fatigue are the most difficult to detect using conventional methods. Several investigations have been reported using vibration-based methods for damage detection. These approaches are more globally sensitive to damage than localized methods such as ultrasonic and eddy current

methods. The use of smart materials for damage characterization and detection has also been widely reported (Doebbling et al., 1996; Schulz et al., 1997, 2003; Ghoshal et al., 1999, 2000; Waldron et al., 2002; Sundaresan et al., 2003). Naturally, the interpretation and accuracy of vibratory responses in identifying damage is dependent on the numbers and types of sensors and actuators that are used. Recently, VDSs are increasingly being used to detect damage (Pandey et al., 1991; McHargue et al., 1993; Doebbling et al., 1996; Richardson, 1997; Schulz et al., 1997, 2003; Chen et al., 1998a,b; Ghoshal et al., 1999, 2000; Schwarz and Richardson, 1999a,b; Sundaresan et al., 1999a,b; Vold et al., 2000; Waldron et al., 2002; Sundaresan et al., 2003). The literature shows the application of Vibration Deflection Shapes (VDSs) for damage detection on bridges, wind turbines, and other structures. The use of VDS for structural damage detection is promising because VDS provides a visual interpretation of the vibration patterns of the structure, thus allowing

*Author to whom correspondence should be addressed.
E-mail: anindya.ghoshal@asu.edu or a.ghoshal@larc.nasa.gov

anomalies to be detected in terms of the geometric features of the structure. A Scanning Laser Doppler Vibrometer (SLDV) can be used to measure the vibration response in a dense spatial pattern to generate VDS and detect small damage. For this purpose, the structure can be excited at the high frequencies necessary to detect small damage by using piezoceramic (PZT) patches or a PZT inertial actuator bonded to the structure. In this paper, VDS is used to detect and localize embedded damage such as delamination and other forms of damage that are near the inner surfaces of composite structures. The outer surface in this paper normally refers to the surface that is used for laser scanning. The term Vibration Deflection Shape (VDS) is used here instead of the more conventional Operational Deflection Shape (ODS) because the ODS can be confused to mean the deflection shape while the structure is under service loads or in operation. The term VDS is used to designate the vibration displacement shape or vibration velocity shape of the structure as measured by the SLDV and displayed by the PSV software. In this paper, vibration displacement shapes are principally used and hence the term VDS is used interchangeably to mean Vibration Deflection Shape and Vibration Displacement Shape.

VIBRATION DEFLECTION SHAPES

In the experimental investigation, Vibration Deflection Shapes obtained using the Scanning Laser Doppler Vibrometer are used for characterizing and localizing the presence of damage. This is based on exciting the structure with piezoceramic patch actuators and measuring the vibratory response using the SLDV. The SLDV system computes VDSs and frequency response functions (FRFs). The VDSs are computed for both the healthy and the damaged structures. Changes in the VDSs are used to indicate and possibly locate damage (Ghoshal et al., 2000; Waldron et al., 2002; Schulz et al., 2003). The following briefly describes how the SLDV uses a complex representation of harmonic vibration to determine the VDS. Details of the derivation can be found in (Ghoshal et al., 2000; Waldron et al., 2002; Schulz et al., 2003).

The equations of motion for a linear structure with periodic excitation can be expressed as follows:

$$M\ddot{x} + C\dot{x} + Kx = \text{Re}(fe^{j\omega_{dr}t}) \quad (1)$$

Defining

$$x(t) = \text{Re}[X(j\omega_{dr})e^{j\omega_{dr}t}] \quad (2)$$

and substitution of (2) into (1) yields:

$$\text{Re}[AX(j\omega_{dr})e^{j\omega_{dr}t}] = \text{Re}[fe^{j\omega_{dr}t}] \quad (3)$$

where $A = (K - \omega_{dr}^2 M + j\omega_{dr}C)$ is the system matrix and $\text{Re}(a+b) = \text{Re}(a) + \text{Re}(b)$ is used, where a and b are some complex constants. Thus, from (3):

$$X(j\omega_{dr}) = Hf \quad (4)$$

where $H = A^{-1}$ is the receptance FRF matrix of the system. The quantity $X(j\omega_{dr})$ in (4) is the frequency domain representation of the system displacement response. Substitution of (4) into (2) gives:

$$x(t) = \text{Re}[Hfe^{j\omega_{dr}t}] \quad (5)$$

The VDS is defined by evaluating (5) at different angles or times during a steady-state sinusoidal response. The angles are:

$$\theta_m = \omega_{dr}t_m \quad (6)$$

where ω_{dr} represents a specific driving or excitation frequency. The VDS can be evaluated at specified angles, $\theta_m = 2\pi m/p$ where p is the number of points in one cycle of vibration to evaluate the VDS and $m = 0, 1, 2, \dots, p-1$. Therefore the time to evaluate the VDS is given by:

$$t_m(\omega_{dr}) = \frac{\theta_m}{\omega_{dr}} = \frac{m2\pi}{p\omega_{dr}} \quad (7)$$

The VDS for displacements can then be written as follows:

$$x\left(\frac{\theta_m}{\omega_{dr}}\right) = \text{Re}[X(j\omega_{dr})e^{j\theta_m}] \quad (8)$$

Similarly, the VDS for velocities can be expressed as:

$$v\left(\frac{\theta_m}{\omega_{dr}}\right) = \text{Re}[j\omega_{dr}X(j\omega_{dr})e^{j\theta_m}] \quad (9)$$

The SLDV uses a periodic chirp excitation and the vibration response is measured for one period of the excitation. A Fourier transform is performed and the complex vibratory response at the particular measurement point is stored. This is repeated for all scan points and the real amplitudes are plotted at selected phase angles. The measured vibration deflection shape approximately coincides with the more familiar mode shape if the mode shapes of the structure are well spaced, damping is small, and the excitation is at a natural frequency of vibration of the structure. It is expected that the VDS will provide more accurate information on damage detection since the exact response of the structure is used, subject only to errors in performing the Fourier transform. On the contrary,

computation of mode shapes involves additional assumptions and procedures, which may magnify the errors and reduce sensitivity for characterizing the effects due to damage.

EXPERIMENTAL INVESTIGATION USING VDS

Noncontact measurements using a Scanning Laser Doppler Vibrometer (SLDV) are used in this experimental investigation for damage detection and localization in composite test structures. Since the velocity resolution of the scanning vibrometer is $0.3 \mu\text{m/s}$, the resulting displacements will have a high level of accuracy necessary for capturing the influence of damage on structural response. The SLDV is used to scan the surface of the composite structures. First, testing is conducted on composite plate-beams with embedded delamination at different ply levels, located near and away from the actuator and of different size. This is followed by the testing of a composite curved plate with delamination near the inner surface (away from the scanning surface), and a honeycomb intertank panel with simulated damage. Periodic chirps or random sweeps are used to excite the composite plate. The SLDV scans the vibration velocity at discrete mesh points and the PSV software computes the displacements and then interpolates between mesh points to plot the structural displacement. To detect and locate damage, the Vibration Deflection Shapes, obtained using the SLDV, are compared for the healthy and the damaged structures. This allows detection of local damage such as cracks or delamination. Global damage such as distributed fatigue damage can also be detected by analyzing the signal from a bonded piezoelectric receiver sensor due to a high frequency burst input from a PZT patch or a shaker. A reduction in stiffness will lead to a frequency shift in the FRFs obtained by the PSV software.

Material Characterization

A set of graphite epoxy laminated composite coupons was prepared for material characterization testing. The fiber used for the laminate is K1100 carbon and the curing resin is 954-2A cyanate resin. It is cured in a Hot Press at 325°F for two hours. The material characterization is done in accordance to ASTM Standards D3039 and D3518. The material properties for the laminated composite are determined to be as follows: $E_1 = 380 \text{ GPa}$, $E_2 = 16.6 \text{ GPa}$, $G_{12} = 4.2 \text{ GPa}$, $\rho = 1800 \text{ kg/m}^3$, $\nu_{12} = 0.31$, $\nu_{23} = 0.42$. It should be noted that the flexural modulus is found to be less than the tensile modulus for laminated composites. In this case, our main interest lies in flexural and twisting

modes, as measured by the SLDV. The in-plane or axial vibration modes are not used in this study.

Experimentation using the SLDV and Carbon Cyanate Laminated Composites

A set of carbon cyanate $(0,90)_{4s}$ laminated composite cantilever plate-beams shown in Figure 1 are manufactured using a Hot Press. The cantilever plate-beams are 31.1 cm long, 5.1 cm wide, and 0.218 cm thick. The ply thickness is measured to be 0.137 mm. One side of the plate-beam is covered with a very thin, flexible laser reflective tape to obtain a better signal-to-noise ratio for the laser measurements. An ACX bimorph PZT patch actuator QP25N is surface bonded about 1.83 cm away from the fixed end of the cantilever plate-beam (Figure 2 (b)). The actuator is attached on the opposite side of the reflective tape. The actuator is located near the fixed end to take advantage of the higher strain field at the fixed end. The size of the actuator is $5.1 \times 2.54 \times 0.051 \text{ cm}$. It consists of two stacked PZT 5H wafers, each of size $4.6 \times 2.1 \times 0.0127 \text{ cm}$. The remaining information including the PZT wafer properties can be found from Cymer ACX manuals, now developed by MIDE Technologies (Cymer, 2001). Coupons are developed for three different cases. Each case consists of four specimens; one being healthy and the remaining three having an embedded delamination in one ply at levels 2, 4, and 7, respectively. In all cases, the delamination is seeded in the half of the plate, from the midplane, that is away from the laser-taped side. Thus, the interfacial ply levels are numbered from the midplane and away from the reflective tape face. The delamination is seeded using two very thin plastic release films placed between the interfaces of two-ply layers. The delamination seeded in Case 1 and Case 2 are of the size $5.1 \times 5.1 \text{ cm}$, whereas in Case 3 it is of the size $10.2 \times 5.1 \text{ cm}$. In Case 1, the closest edge of the delamination is located 15 cm from the free end, in Case 2 it is 23 cm away from the free end, and in Case 3 it is 12.4 cm away from the free end. All of the delaminations are centered widthwise.

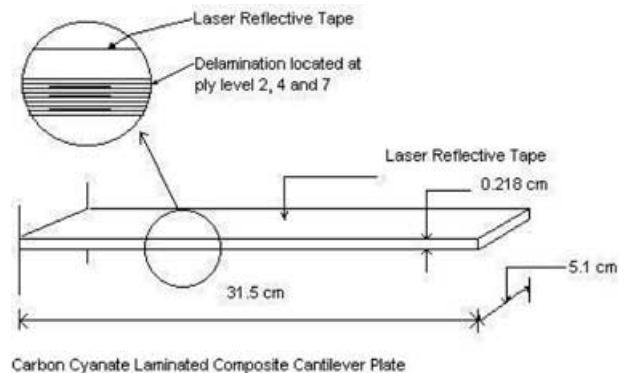


Figure 1. Carbon cyanate laminated composite cantilever plate with delamination.

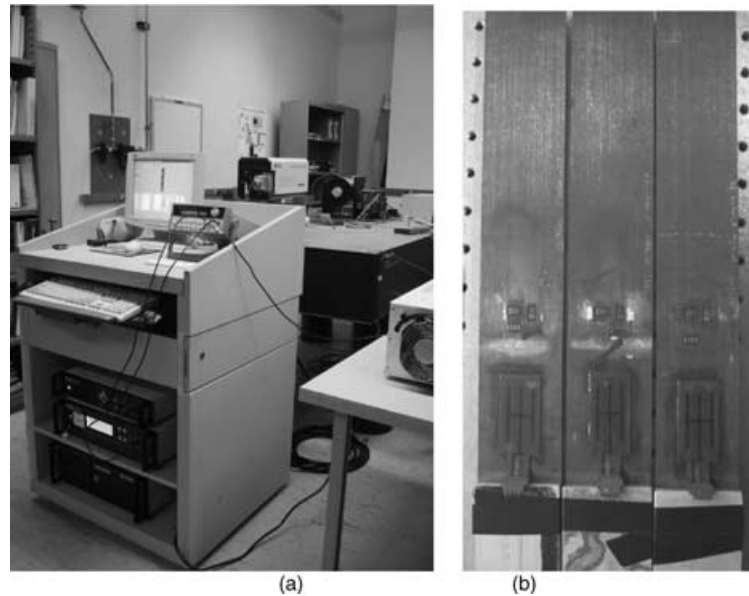


Figure 2. (a) Experimental setup for laser vibrometry testing; (b) A set of laminated composite cantilever plate-beams with ACX PZT actuators (QP25N) attached near the fixed end.

The experimental setup for the laser vibrometry testing is shown in Figure 2(a). The setup consists of a cantilever plate-beam with a surface bonded ACX QP25N bimorph actuator mounted on a vice attached to a Newport RS4000 vibration isolation table, a Polytec SLDV, an Agilent 33120A waveform generator, and an ACX Quickpack Power Amplifier. The piezoelectric PZT patch actuator mounted near the fixed end of the cantilever plate is used to excite the structure while the laser scans the outer surface for transverse vibration and displacement. It must be noted that a slight offset in the placement of actuator from the centerline of the beam along the width (lateral) direction is used to generate both bending and torsional modes, although the flexural modes are predominant in terms of amplitude produced. It is also expected that a perfect clamped/fixed end is not possible to simulate experimentally, hence a partially restrained boundary condition can also be effective in producing both flexural and torsional modes.

QUASI-STATIC TESTING OF COMPOSITES USING SLDV

Quasi-static testing using the SLDV is conducted to determine if the composite specimens are identical in dimensions and material properties without having to do material characterization and computational modeling. The surface bonded PZT patch on the cantilever composite plate is actuated using a very low frequency 0.5 Hz square wave input of 7.5 V with a gain of 20 (total input voltage = 150 V). This enables the SLDV to measure the static tip displacement of all four specimens, individually, for each of the three cases using a single shot measurement technique. Displacement versus

frequency FRF graphs plotted by the PSV software show that the magnitude of the maximum displacement of the four specimens, for each of the three cases, lie within the range of 100 and 105 μm at 0.5 Hz (Figure 3 is one such example). The difference in the measured responses is less than 5%. This quasi-static test using a low frequency square wave with a controlled input voltage is performed to ensure the identical nature of the specimens in terms of dimensions and material property. This quick quasi-static testing is important to ensure that all the specimens used in the experimentation are identical in dimensions and material properties.

DELAMINATION DETECTION IN LAMINATED COMPOSITES USING VDS

Experimental investigations have been conducted using the above mentioned carbon cyanate laminated composite cantilever plate-beam specimens with seeded delaminations (Figure 2(b)) using the Scanning Laser Doppler Vibrometer (SLDV). The experimental setup is shown in Figure 2(a). It is important to note that the amplifier should be moved away from the isolation table as the noise of the fan of the amplifier may affect laser readings. The experimental method involved exciting the structure initially with broadband periodic chirp inputs or sine sweep inputs and then scanning the structure with the laser. The FRF plots identify the natural frequencies of the structure and the corresponding VDS are analyzed. In doing so, the VDS for particular frequencies where distortions caused by the presence of damage or other anomalies are identified. Then either the structure is excited with a sine input at those specified frequencies or the bandwidth of the periodic chirp is narrowed considerably and the laser scan mesh

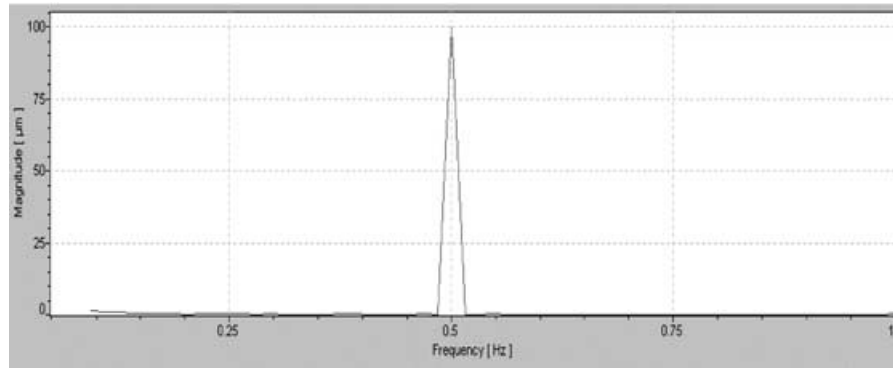


Figure 3. A typical FRF showing the magnitude of the tip displacement of the cantilever plate-beam due to a 0.5 Hz square wave excitation, which has an input voltage of 150 V.

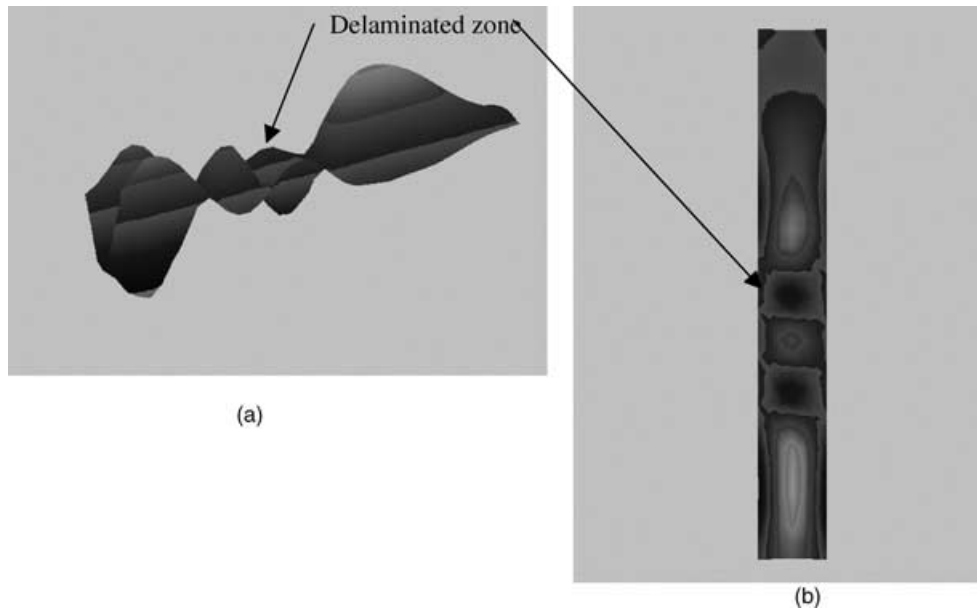


Figure 4. Laser VDS showing the vibration distortions caused by delaminations.

is also made denser. This is done to increase the input excitation energy to enhance the effect of the damage on the distortion of the VDS and also for a greater signal-to-noise ratio. Preliminary results from laser scans are analyzed to assess the effectiveness of VDS in detecting and locating delamination. Figure 4(a)–(b) presents a typical laser vibration deflection shape (VDS), showing vibration distortions caused by the presence of delamination. Next, experiments are conducted to investigate issues such as placement of actuator with respect to the delamination location, on the structure, size of the delamination, and location of the delamination for the VDS method to be effective in detecting and locating the extent of damage. It must be noted that the following set of experiments were performed within the frequency band of 1 Hz–20 kHz for this particular material (Cases 1–3). Higher bandwidth excitation (exceeding 20 kHz) led to noisy laser readings and a much lower signal-to-noise ratio and hence those results are not presented in this study.

Effect of the Through-the-thickness Position of the Delamination

The effect of delamination location, through the laminate thickness, is studied in the following experiments for Case 1 using a set of four specimens. The details of these specimens have already been described previously. The details of the experimental process using the SLDV have been mentioned there.

(a) Natural Frequency Comparison: Normally the natural frequency shift between a healthy and a damaged structure is caused by the presence of a large amount of damage or due to distributed fatigue. The natural frequency shift is a global indicator of the presence of damage. Analytical results, obtained using a higher order theory (Thronburgh et al., 2002), also show that useful information can be obtained from the natural frequency comparison in the case of local delamination damage. Figure 5 shows the FRF comparison for the frequency bandwidth of 1–1000 Hz for the

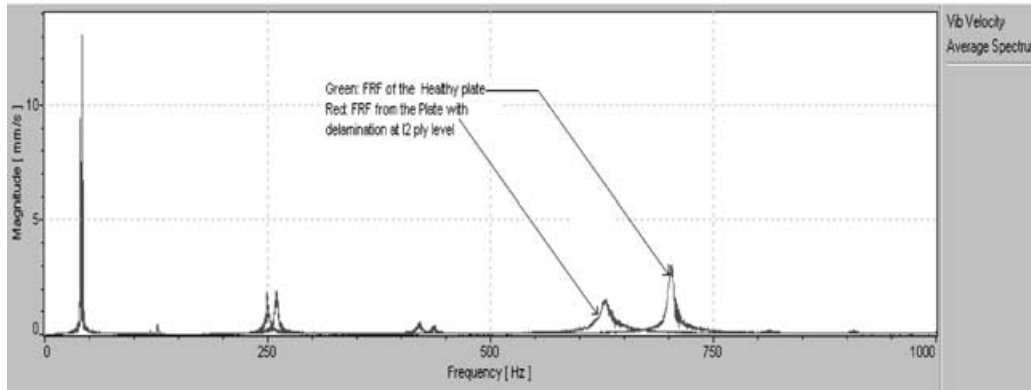


Figure 5. FRF comparison for the frequency bandwidth of 1–1000 Hz for the Healthy and Damaged Plate with a delamination at the interfacial ply level I2.

healthy and the damaged plate with a delamination located at ply level I2 for Case 1. The FRF peaks denote the natural frequencies of the laminated composite specimen. The frequency shift due to the presence of delamination is clearly noticeable and becomes more pronounced in higher modes. Table 1 presents the first five natural frequencies of the composite plate obtained using a four-node finite element (FE) model with 30×5 elements for Case 1. The numbers I2, I4, and I7 denote the presence of delamination at that layer. Once again, the ply level is measured from the midplane ($n = 1$) and away from the surface, which has the reflective tape attached to it. Table 2 presents the experimental values of the first five natural frequencies, obtained from the SLDV, for both the undamaged and the delaminated cantilever plate-beam samples. Comparison of the natural frequencies in Tables 1 and 2 show that the numerical and the experimental results are within 8% of each other. The discrepancy can be due to the slight variance in the material properties obtained from the material characterization studies. This investigation shows that the natural frequency shift between the healthy and damaged structure is more pronounced at: (i) higher frequencies, and (ii) when the delamination is embedded nearer to the midplane of the composite laminate. Therefore, although the frequency shift, which is caused by changes in structural stiffness, is generally not a good indicator of local damage, it appears that identification of the high frequency modes can be useful since they affect the VDS locally.

The pronounced natural frequency shifts when the delamination is near the midplane rather than when near the surface of the laminated composite with respect to the healthy structure can be empirically understood by computing the bending inertia. Assuming that the delamination causes sliding on the two delaminated surfaces, one can compute the bending inertia for delamination near the surface of the composite and at the center of the composite. For example, $I(\text{healthy}) = bh^3/12 = 0.083bh^3$,

Table 1. The first five natural frequencies obtained from a four noded plate finite element model of case 1 consisting of 30×5 elements of the composite plate.

Natural Frequencies (Hz)	Undelam (Hz)	I7(Hz)	I4(Hz)	I2(Hz)
ω_1	42.08	42.06	41.96	41.89
ω_2	133.9	133.5	132.4	131.4
ω_3	260.2	259.5	258.9	258.4
ω_4	457.6	453.6	455.7	455.4
ω_5	717.4	695.8	692.0	678.4

Table 2. The first five natural frequencies obtained from experimental values using laser vibrometry for the undelaminated and delaminated cantilever beam plate-beam samples for case 1.

Natural Frequencies (Hz)	Undelam (Hz)	I7(Hz)	I4(Hz)	I2(Hz)
ω_1	41.26	40.94	40.31	40.0
ω_2	125.8	122.7	120.8	118.3
ω_3	255.1	250.6	250.6	249.4
ω_4	434.0	430.8	421.7	420.6
ω_5	703.8	690.6	639.5	628.6

$I(\text{delamination at } 1/8 \text{ from top}) = (bh^3/12)((7^3/8^3) + (1/8^3)) = 0.056bh^3$, $I(\text{delamination at center}) = (bh^3/12) \times ((1/2^3) + (1/2^3)) = 0.0208bh^3$. This shows that the delamination near the surface reduces the inertia by 33%, while delamination at the center reduces the second area moment of inertia by 75%. This assumes sliding of the surfaces at the delamination, and only is accurate for a delamination along the full length of the composite plate-beam. Natural frequencies for the structure are proportional to the square root of the stiffness, i.e., since Young's modulus E is constant, thus the natural frequencies are directly proportional to the square root of the bending inertia of the structure. Therefore, the natural frequencies are reduced by 25% when the delamination is at 1/8 from top, while when the delamination is at the center, it is reduced by 50%. It is less in the experiments because

it does not fully satisfy the assumption made in this preliminary analysis.

Figure 6 compares the ratio of the delaminated (w_d) and healthy fundamental natural frequencies (w_h) for the composite plate-beam (obtained using a FEM model consisting of 10×4 four node plate elements and an improved layerwise theory (Kim et al., 2001)) and the square root of the ratio of the moments of inertia for delaminated (I_d) and healthy beams (I_h). The size of the composite plate is 30 cm in length, 5 cm in width and 0.218 cm in thickness. The material properties are the same as described previously. The I_0, \dots, I_7 denotes the ply at which the delamination is considered to be present. It is assumed that the delamination is present throughout the full length of the composite plate. In this case of full-length delamination, it is possible hence to get the ply level information if the fundamental frequencies of the delaminated plate and the undelaminated plate can be ascertained. By comparing the ratio of w_d/w_h and comparing with the I_h/I_d graph, one can deduce the ply-level information. However the analysis would be far more complicated for ply level localization

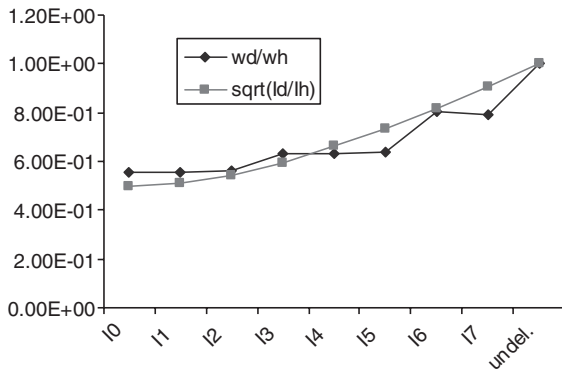


Figure 6. Comparison of the ratio of the delaminated (w_d) and healthy fundamental natural frequencies (w_h) for the composite plate-beam (obtained using a FEM model consisting of 10×4 four node plate elements and an improved layerwise theory (Kim et al., 2001)) and the square root of the ratio of the moments of inertia for delaminated (I_d) and healthy beams (I_h).

for delamination of arbitrary sizes. This is an empirical way of understanding the change in natural frequencies due to the presence of delamination at different ply level interface. Detailed theoretical calculations are needed to prove it analytically especially when trying to locate the ply-level information for delamination of arbitrary size. It is experimentally later shown in this paper how delamination can inhibit transference of flexural energy along the length of the plate for certain frequency bands.

(b) *Effect on Vibration Displacement Shapes:* Figure 7(a)–(d) shows the vibration displacement shapes (VDS) at the fundamental frequencies of the cantilever plate-beam with no delamination and with delamination of length 5.08 cm at ply levels I_7 , I_4 and I_2 , respectively (Case 1). The natural frequencies are presented in Table 2. No discernible effect of delamination is observed on the VDS of the cantilever plate-beams, which means that low frequencies are not very useful in characterizing the effect of delamination on the VDS. Figure 8(a)–(d) presents the associated vibration displacement shapes (VDS) at a higher mode. The natural frequencies of the delaminated plate in this case are 4.241, 4.005, and 3.689 kHz, respectively. The effect of delamination is now observed on the VDS of the cantilever plate-beam. The distortion in the VDS increases significantly as the delamination is embedded closer to the midplane. However, the effect of distortion is still global and therefore localization of the area of delamination is not yet possible. Figure 9(a)–(d) shows the vibration displacement shapes (VDS) at another higher mode with natural frequencies of 9.084, 8.841, 8.664, and 8.273 kHz, respectively, for the four delaminated test cases. Once again, the effect of delamination is observed on the VDS. In fact, there is complete loss of one half of the wavelength in the beam with delamination located at ply level I_7 (Figure 9(b)) compared to the healthy one (Figure 9(a)). Again, the distortion in the VDS is significantly greater as the delamination moves closer to the midplane. In the case of delamination

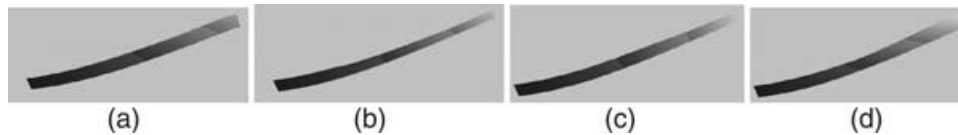


Figure 7(a)–(d). This shows the vibration displacement shapes (VDS) at the fundamental frequencies of the cantilever plate-beam (Case 1) with no delamination and delamination of 5.08 cm at I_7 , I_4 , and I_2 ply levels respectively. The natural frequencies are given in Table 2, row 1.

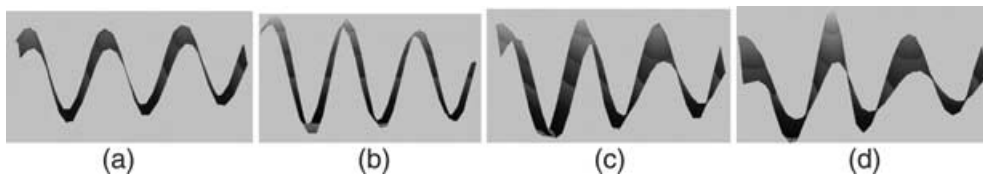


Figure 8(a)–(d). This shows the vibration displacement shapes (VDS) at a higher mode of the cantilever plate-beam (Case 1) with no delamination and delamination of 5.08 cm at I_7 , I_4 , and I_2 ply levels respectively. The natural frequencies for this particular mode for the four coupons are 4.387, 4.241, 4.005, and 3.689 kHz, respectively.

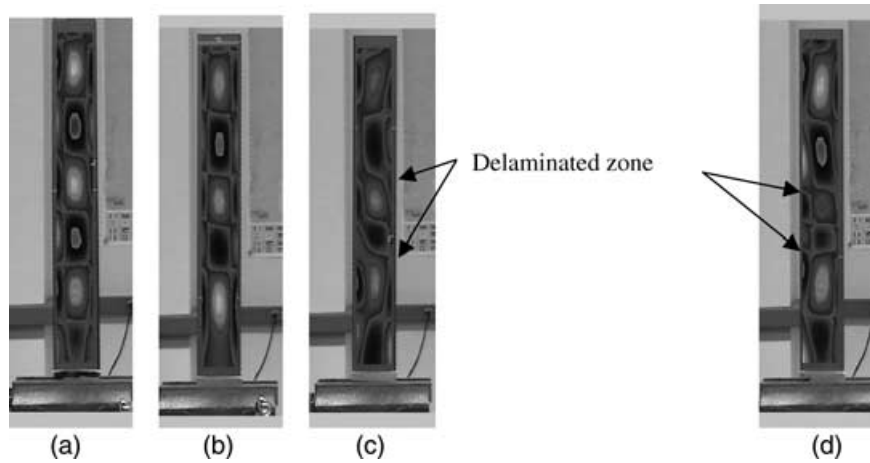


Figure 9(a)–(d). This shows the vibration displacement shapes (VDS) at a higher mode of the cantilever plate-beam (Case 1) with no delamination and delamination of 5.08 cm at 17, 14, and 12 ply levels respectively. The natural frequencies for this particular higher mode for the four coupons are 9.084, 8.841, 8.664, and 8.273 kHz, respectively.

located at ply levels I4 and I2 (Figure 9(c) and (d)), the delamination zone is clearly identifiable. This effect is similar to the natural frequency characteristics at higher frequencies. It is also important to note that in this case the delamination closer to the midplane is also closer to the surface bonded actuator. Thus, the VDS, coupled with the natural frequency shift information from the healthy and damaged body data, can detect the presence of delamination, localize the area of delamination in the plane of the surface, and indicate the location of the delamination with respect to the thickness of the laminate. However, it does not provide the information about the exact ply level location of the delamination. It is expected that more detailed post processing of the VDS information may provide more accurate information regarding ply level location of the delamination.

Effect of Pure Bending Modes as Opposed to Twisting Modes

Figure 10(a) shows the VDS for the fifth twisting mode of the cantilever plate-beam with no delamination, and a delamination of size 5.08 cm, located at ply levels 17, 14, and 12, respectively, for Case 1 specimens. The natural frequencies for this particular higher mode for the 4 (delaminated) coupons are 2.440, 2.344, 2.248, and 2.145 kHz, respectively. The distortion effect in the VDS due to the presence of delamination is noticeable in the cases with delamination located at ply levels I4 and I2. It is clearly localizable in the VDS of the I2 ply delamination cantilever beam-plate, which in effect reinforces the earlier conclusion that the closer the delamination is seeded to the midplane, the easier it is to detect and locate its effect using low frequency modes. The vibration displacement shapes (VDS) for the fifth bending mode, of the same specimens, are shown in Figure 10(b). The natural frequencies for this particular higher mode for the four delaminated coupons are

2.195, 2.123, 2.004, and 1.856 kHz, respectively. The distortion effect in the VDS due to the presence of delamination is noticeable in case of the I4 and I2 ply delamination cantilever beam-plates. In lower frequency flexural modes VDS global effects like change in amplitude are normally observable. However, unlike the twisting mode, the VDS do not allow localization of delamination for the case with delamination located at ply level 12. This indicates that damage localization may be easier through observation of the VDS associated with the twisting mode as opposed to the bending mode, particularly at lower frequencies. Similar observations have also been made in (Waldron et al., 2002). This observation is made with the caveat that the amplitude of the VDS for a particular twisting mode is smaller and more difficult to measure than for the corresponding bending mode.

Effect of the Distance Between the Actuator and the Delamination

This comparison is conducted between Case 1 and Case 2 specimens with a delamination of size 5.1×5.1 present at ply level I2. As noted before for the Case 1 specimen, the delamination is located 15 cm away from the free end, whereas for the Case 2 specimen the delamination is seeded 23 cm away from the free end. For the Case 2 specimen, it must also be noted that the delamination falls partly under the PZT actuator, which is surface bonded to the plate-beam. Figure 11(a) shows the second twisting mode for the Case 1 specimen at a frequency of 420.6 Hz. Figure 11(b) shows the same mode for Case 2 at a frequency of 410.8 Hz. These figures clearly indicate that distortion in the VDS due to the presence of the underlying delamination is observable in Case 2. Hence it is inferred that for this low frequency mode VDS comparison, it is easier to detect the effect of delamination on the VDS when the actuator is located closer to the delamination. Figure 12(a) shows

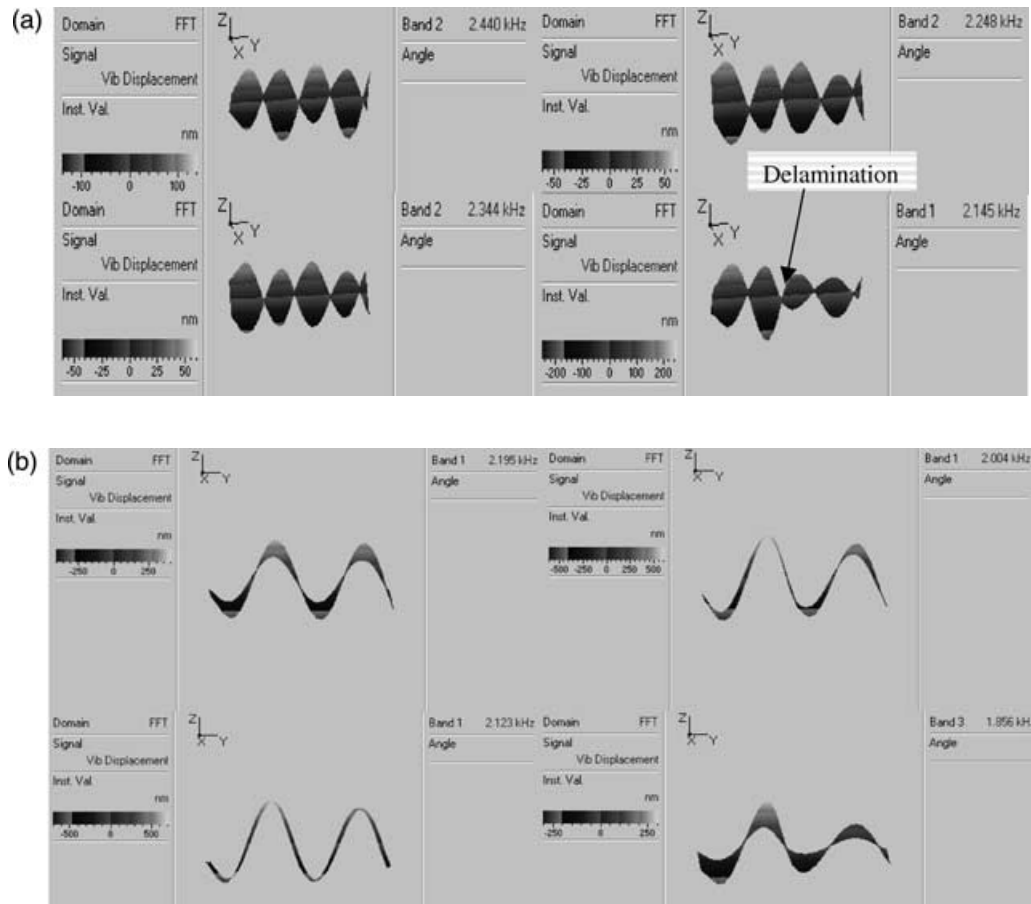


Figure 10. (a) This shows the vibration displacement shapes (VDSs) for the fifth twisting mode of the cantilever plate-beam with no delamination (top left figure) and delamination of 5.08 cm at I7 (bottom left), I4 (top right) and I2 ply (bottom right) levels respectively. The natural frequencies for this particular higher mode for the four coupons are 2.440, 2.344, 2.248, and 2.145 kHz, respectively; (b) This shows the vibration displacement shapes (VDSs) for the fifth bending mode of the cantilever plate-beam with no delamination (top left figure) and delamination of 5.08 cm at I7 (bottom left), I4 (top right) and I2 ply (bottom right) levels respectively. The natural frequencies for this particular higher mode for the four coupons are 2.195, 2.123, 2.004, and 1.856 kHz, respectively.

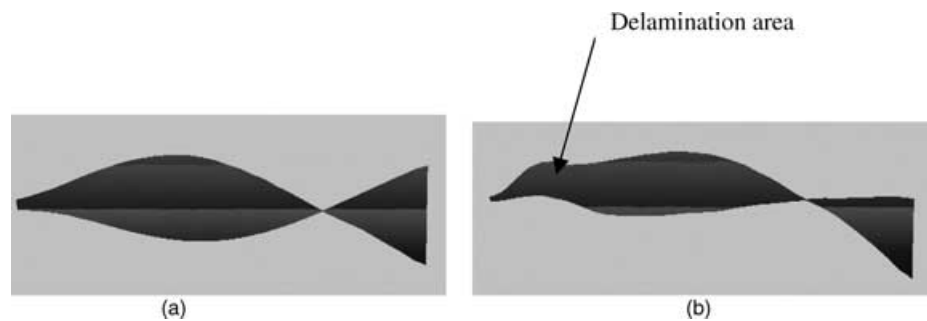


Figure 11. (a) Second twisting mode for case 1 specimen (I2 ply level delamination away from the actuator) at 420.6Hz; (b) Second twisting mode for case 2 (I2 ply level delamination near the actuator) at 410.8Hz.

a higher frequency, flexural mode, VDS for Case 1 (frequency of 4.952 kHz) and the same information is presented in Figure 12(b) for the Case 2 specimen (frequency of 4.964 kHz). In the high frequency VDS, for both cases studied, the planar outline of the delaminated zone is clearly identifiable. It is obvious that for both cases the localization of the planar area of the delamination is easier using the high frequency VDS.

However, for the Case 2 study, it is important to note the distinction between the VDS due to PZT actuation only on the healthy structure and the distortion caused by presence of the underlying delamination. Figure 12(c) shows the VDS for the healthy case at 5.466 Hz, where the effects of PZT actuation are clearly identifiable. The VDS presented in Figure 12(b), for the damaged structure, shows the additional distortion due to the

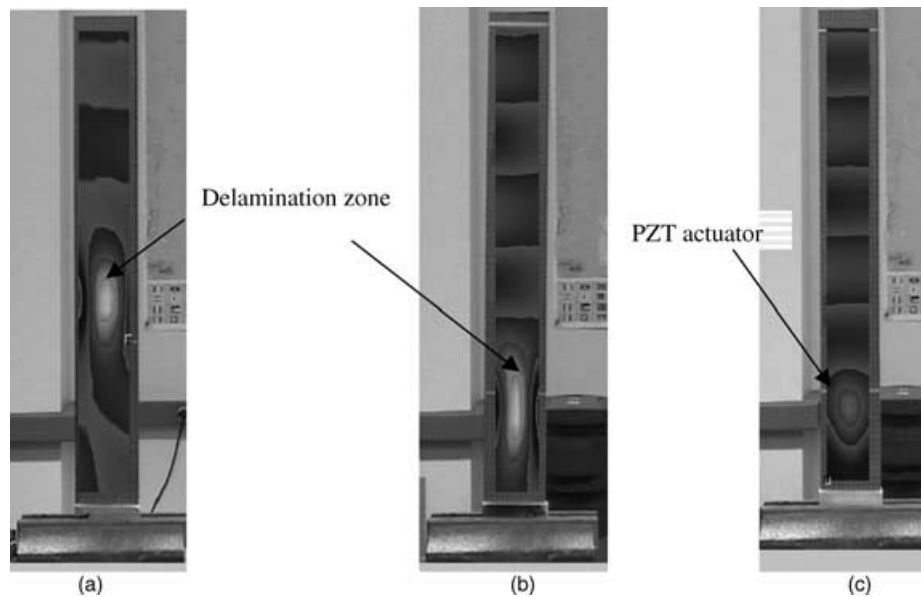


Figure 12. (a) Higher frequency VDS of case 1 at 4.952 kHz. Note the outline of the delaminated zone is clearly identifiable; (b): Corresponding higher frequency VDS of case 2 at 4.964 kHz. Note the outline of the delaminated zone is clearly identifiable; (c) The corresponding VDS for the healthy case at 5.466 Hz, where the outlines of the PZT actuation is clearly identifiable; (b) shows the distortion due to presence of underlying delamination on the healthy PZT actuation VDS.

presence of the underlying delamination. The difference is clearly noticeable.

Effect of the Size of the Delamination

Next, comparison is made between the delamination present at ply level I2 for two specimens with differing delamination size; 5.1×5.1 cm in Case 1, and 10.2×5.1 cm in Case 3. In both cases the centerline of the delaminations are located at a distance of 17.5 cm away from the free end but the edges of the delaminations are 15 and 12.4 cm away from the free end, respectively. In Case 1, the VDS corresponding to the low frequency modes (Figures 7(d) and 11(a)) do not show the effect of delamination. However, the VDS for the higher frequency modes can still identify the delaminated zone in the planar view (Figures 8(d), 9(d), 12(a)). Figure 13(a) and (b) present the VDS for Case 3 at a frequency of 74.8 and 116.4 Hz, respectively. Figures 13(c) and 13(d) show the surface planar and 3-D contour view of the VDS for the Case 3 specimen at a high frequency of 4.835 kHz. It is observed that the effect of delamination is observable in all of the VDS shown in Figure 13 (a)–(d). However, the damage is localizable in the higher frequency VDS. Therefore, as expected, a larger size delamination is easier to detect even using the lower frequency VDS. However, the higher frequencies are needed for the detection and localization of smaller delamination.

Effect of Actuator Integrity and Nearby Delamination

Figure 12(c) shows a typical VDS of the healthy beam under actuation at 5.446 kHz. The location of the piezoelectric actuator is clearly identifiable near the

fixed end when the beam is excited at this frequency, as shown in Figure 12. Likewise, there are certain frequencies where the actuating PZT patch can be identified. However, if there are problems with actuator integrity, such as disbonding, or there is an underlying delamination or other form of damage present in the composite host structure below the actuator, the VDS would appear distorted as shown in Figure 12(b) and in Figure 14(a). Thus, the actuator integrity or the presence of damage below the actuator can be tested using a historical data set for comparison. As mentioned before, it is important to first identify and distinguish the local effect of the actuator on the VDS before determining the effect of the underlying delamination or other damage present in the structure. More detailed investigation is necessary for establishing a clear-cut experimental methodology for application of the VDS technique to distinguish between the two effects.

Effect of Delamination on Energy Absorption

An interesting phenomenon has been observed during the course of experimentation with the VDS. It is found that for certain frequencies and frequency bands, the presence of the delamination reduces the transfer of the flexural moment and energy from the actuator, which is located on one side of the delamination, to other side of the delamination, as shown in Figure 14(a) and (b). It can be clearly seen from the VDS that the amplitude of flexural vibration on part of the cantilever plate-beam decays significantly. This phenomenon is not observed at other frequencies. It must be noted that in the present case, the VDS is plotted for only the natural frequencies

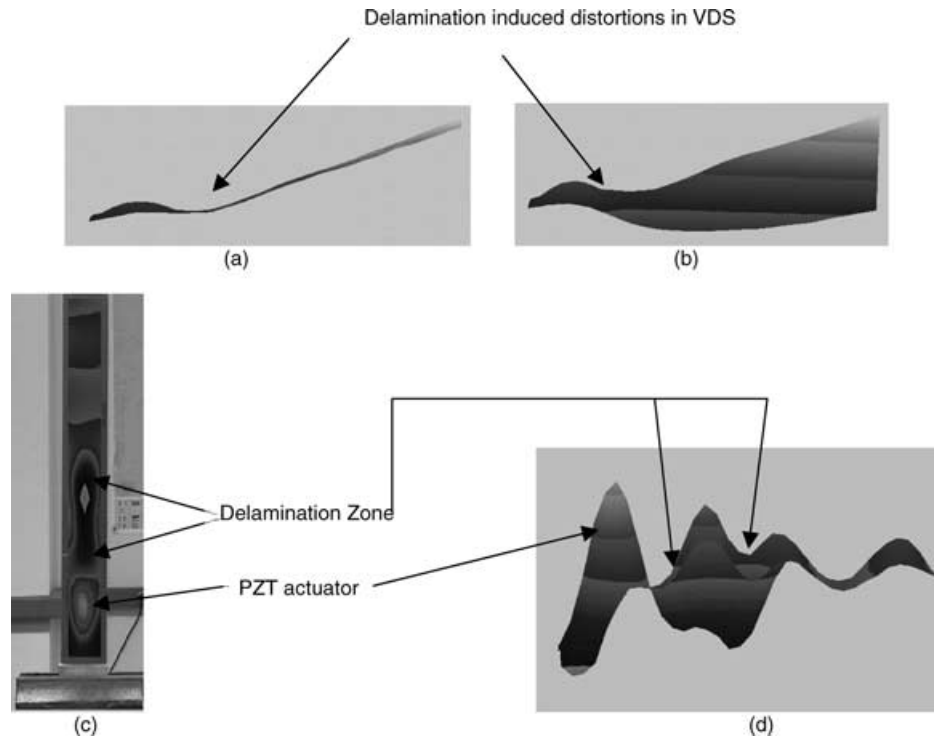


Figure 13. (a) VDS of case 3 (ply level I2 delamination) at frequency 74.8 Hz; (b) VDS of case 3 specimen at 116.4 Hz, (c) and (d) planar and 3-D contour view of the VDS of case 3 specimen at 4.835 kHz. It is observed that the effect of delamination is observable in all of the VDS shown in Figure 13(a)–(d). However, it is only localizable in the higher frequency mode VDS as shown in (c) and (d).

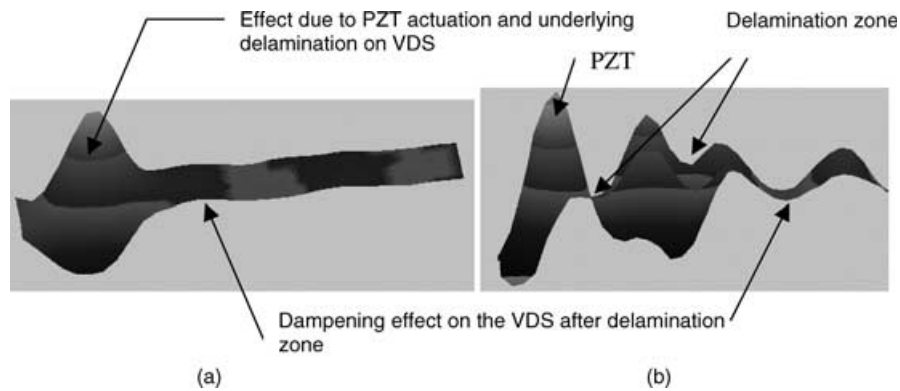


Figure 14. (a) VDS of case 3 at frequency 4.579 kHz; (b) VDS of case 3 at frequency 4.835 kHz.

and therefore this phenomenon is different than mixed mode or complex VDS, which are observable when the VDS is obtained at a frequency that is influenced by two or more closely spaced natural frequencies. This gives rise to the possibility that the delamination is causing pass and stop bands for the frequencies, acting like a filter by absorbing energy from certain frequency bands. This can have many potential applications in practical composites engineering problems where energy absorption is a key issue. For example, the presence of seeded multiple delamination, at different layers, can help absorb energy due to impact in armored vehicles and in bulletproof vests. Further investigation is necessary to validate this observation before such definitive conclusions can be drawn.

Delamination Detection in a Curved Fiberglass Panel

The following two experimentations are carried out on large structures, keeping in mind possible industrial applications for the use of the VDS method for damage detection and localization. In Figure 15(a)–(d), a delamination on the inside of a curved fiberglass panel of dimension $48'' \times 48'' \times 1/4''$ is detected by the SLDV by scanning over the outer surface. The delamination as shown in Figure 15 (a) and (c) is located on the opposite side of the scanned surface. Simultaneous actuation by two PZT (QP10N) patches (located as shown in Figure 15(a)) and a sine excitation at 14.81 kHz (with input voltage of 200 V) are used to excite the panel and the measured displacement at the delamination is 31 nm.

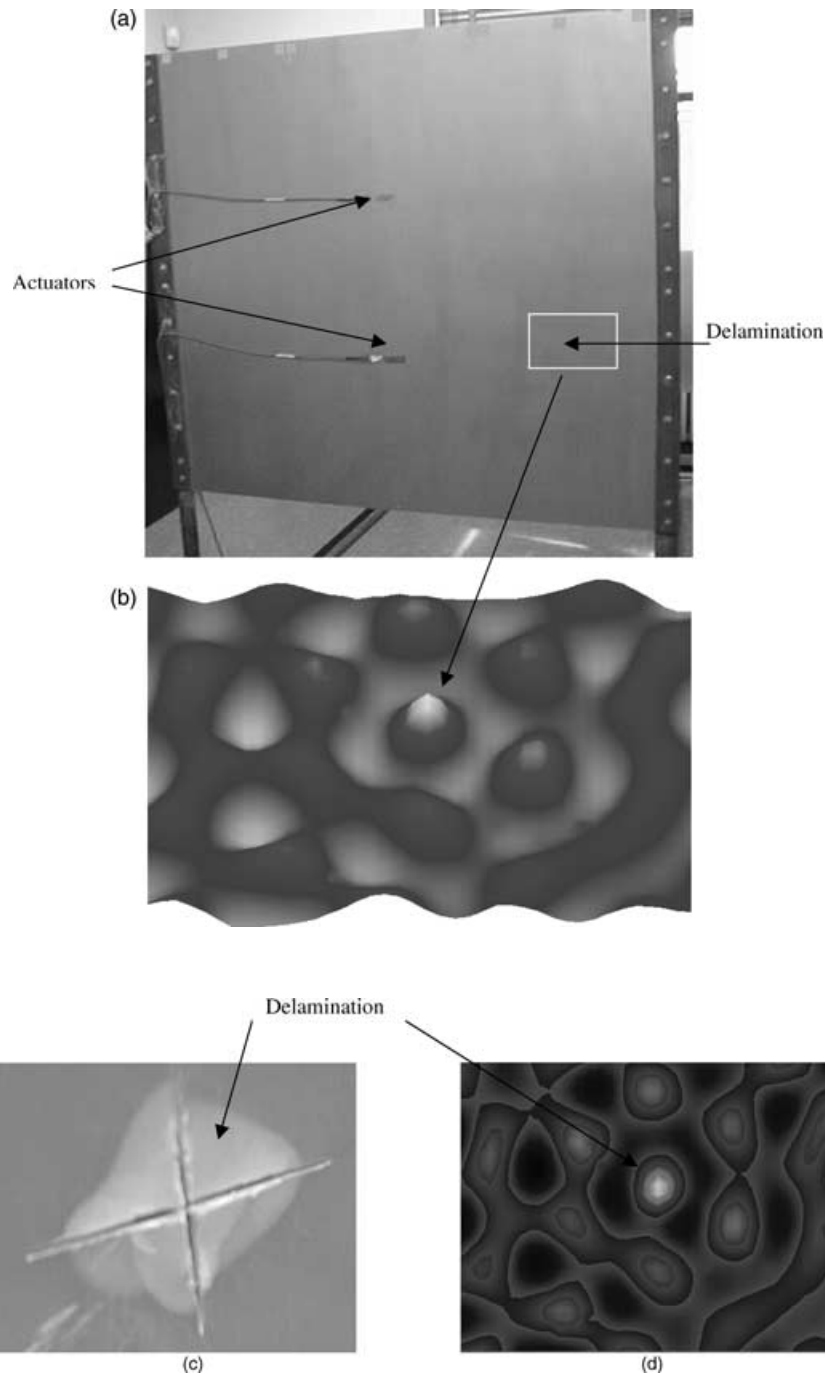


Figure 15. (a)–(d) SLDV scan showing hidden delamination on a curved fiberglass panel at 14.81 kHz.

Figure 15(b) and (d) shows the planar location of the delamination determined from the VDS of the curved panel. The test procedure requires first scanning the structure at different frequency bands using a wide band chirp input to identify the resonant frequencies, and then exciting at these individual frequencies using a sine wave. The initial testing required a lot of time scanning at different frequencies to determine the optimal excitation frequency to detect the delamination while maintaining a satisfactory signal-to-noise ratio. The sine excitation puts the maximum energy into the structure

at resonance, and the peak point of the VDS identifies the damage site.

Damage Detection in a Honeycomb Graphite Epoxy Panel

The application of damage detection using VDS and piezoceramic (PZT) patches to generate periodic waves and the laser vibrometer to scan the surface of the structure and to measure the propagating waves in the structure is now investigated for a large structure. In

large structures, waves travel from the source outward and over the structure. The patterns and amplitudes of these waves propagating over the structure can indicate the internal geometry of the structure and hidden damage. High frequency excitation and sensing produce the greatest sensitivity and predamage data aids in the visual indication and interpretation of damage for complex structures.

A graphite epoxy honeycomb booster intertank panel (8 ft \times 2.5 ft \times 1 in. thick and curved) is used for the experimentation. A battery of preliminary testing with the SLDV was performed to find a suitable method for damage detection in the panel. A PCB power amplifier (model 790 series) and a high power ENI Model 2100RF Power amplifier were used to drive the actuator (QP10N) to its maximum limit of 200 V, but did not produce a satisfactory excitation, except in an area local to the PZT actuator. The experimentation showed that the honeycomb structure is highly damped and a very stiff material. Hence, commonly used PZT actuators (2" \times 1") and piezo-inertial actuators were not able to actuate the structure globally such that the scanning laser vibrometer could measure the panel vibration and wave propagation response with a high signal-to-noise ratio at high frequencies. For such a highly damped material to have sufficient vibration amplitude and to be able to drive a piezoceramic actuator at high frequencies, higher actuation authority becomes imperative. Therefore, new high-power instrumentation was purchased and a series of experiments had to be performed to establish new testing parameters for the intertank panel. These experiments are described next.

EXPERIMENTAL SETUP

An Inter-Digitated Electrode (IDE) PZT (2" \times 1", QP10Ni) actuator patch, which has a 50% higher d_{33} coupling coefficient than the QP10N patches used previously and produces unidirectional actuation was used to excite the panel. Although both QP10N (baseline actuator) and QP10Ni have the same geometry, the following are the differences between the two: (1) The interdigitated electrodes enable directional actuation, rather than planar isotropic actuation; (2) the effective d_{33} parameter is higher than the d_{31} as mentioned earlier, thus the coupling coefficient is higher; (3) for the same driving field, i.e., 200 V for 10 mil baseline actuator or 1200 V for the IDE patch with 60 mil spacing, the average driving fields are equal and the expected increase in actuation authority is a factor of 2. In this context, it must be mentioned that stacked PZT actuators or arrays of PZT actuators would definitely provide increased actuation authority and might prove very useful in detection of internal damages. However they would change weight of the structure (which maybe a concern for lightweight space structures) and affect the local structural behavior more than a single

QP10Ni. Usage of arrays of PZT actuators in this case might make detection of internal damages more difficult than when using only one QP10Ni because of the local distortion in the VDS caused by the actuators (as shown before). Also as noted later, directional actuation actually do help in enhancing the performance in this particular example.

This IDE patch can be driven at an actuation voltage of 1200 V instead of the 200 V maximum voltage limit in conventional PZT patches. To drive the patch, a TREK High Voltage Amplifier (HVA) was used. A waveform generator (HP 33120 A) signal with amplitude of 5 V was amplified to 1000 V using the TREK HVA. Proper precautions are needed for the testing at this high voltage level. The amplifier should not be operated when the relative humidity is higher than 75%. Specially obtained high voltage wires from TREK had to be used for connecting and grounding. The high voltage output from the amplifier is attached to a BNC cable, which is connected to the IDE PZT actuator.

Figure 16 shows the intertank panel being tied to a truss frame to isolate it from ambient room vibration. The intertank panel was painted with silver-white reflective paint obtained from Axon Aerospace to increase the reflectivity for the laser. The actuator is surface bonded to the panel using superglue. It should be noted that the patch is bonded in the center of the panel, which is helpful in actuating the panel symmetrically to obtain the VDS due to the electrode pattern and induced electric field direction. The IDE patches are unidirectional in their actuation (in this case, it actuates the panel in the x -direction which is horizontal and parallel to the long direction of the panel). Note that the Poisson ratio effect will cause some second order actuation in the transverse direction also. The BNC cable can carry up to 3000 V max and the IDE PZT patch can drive at a maximum level of 1200 V. However, a specific fatigue life-period of the IDE PZT patch at high voltage was not available, and the patch itself is in a preliminary design stage. The BNC cable is then grounded to the amplifier, which provided a connection for grounding. In order to simulate reversible damage, a small mass (2 \times 2 \times 0.25 in.³ steel) was bonded to the back inside surface of the honeycomb panel, which is to the right side of the IDE actuator. The actuator is placed on the front side which is the same side scanned by the laser. Figure 17 shows the mass attached at the back surface of the panel (which is away from the scanning surface) to simulate reversible damage.

EXPERIMENTAL RESULTS AND DISCUSSION

Using broadband periodic chirp sweeps, FRF graphs are obtained from laser scans. The peaks in the FRF graphs represent the natural frequencies of the structure. Similar peaks can be obtained using a sine sweep. The VDS for different natural frequencies are plotted.

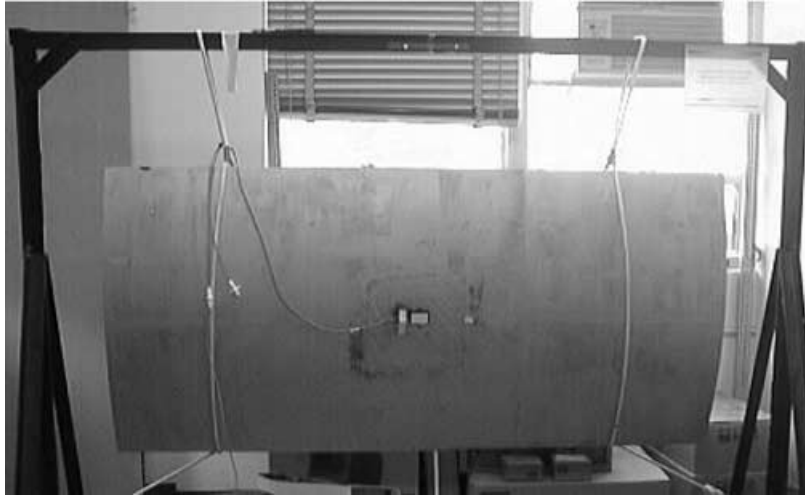


Figure 16. The intertank panel suspended by ropes with the IDE actuator in the center.

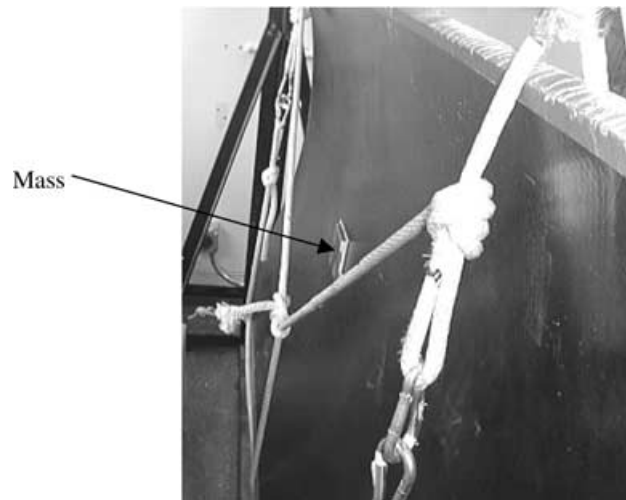


Figure 17. Back view of the panel suspended by ropes with the mass attached to simulate damage.

Depending on the anomalies in the VDS of the damaged honeycomb graphite epoxy panel, selected frequencies are chosen for sine actuation to put more energy into the panel at those particular frequencies. Figure 18 shows the Isoclines and Contour of the VDS of the curved panel due to periodic chirp actuation at 217.2 Hz. This is the first (lowest frequency) VDS for the curved panel, which is behaving like a vibrating curved plate under low frequency vibration. The deflection amplitude is higher at low frequencies, but anomalies in the VDS or loss of symmetry due to the presence of the damage (added mass at the inner surface of the panel) are not observable.

Figure 19 shows the figure of the VDS due to sine excitation at 2.781 kHz. Note that the effect of the IDE PZT patch actuation and the added mass as simulated damage are observable as circular regions that do not propagate with the traveling vibration deflection waves. This establishes the effectiveness of the VDS method as a method for Structural Health Monitoring of the

Honeycomb graphite-epoxy curved panel without historical data.

Figure 20(a) shows the VDS of the panel due to periodic chirp actuation at 5.122 kHz and Figure 20(b) shows the VDS of the panel due to sine actuation at 5.341 kHz. In both types of actuation, chirp, and sine, the loss of symmetry due to the presence of the added mass is found to be observable, whereas the localization of the damage area is more clearly observable in Figure 20(b), which shows the VDS of the curved panel due to sine actuation. This result is improved because of the higher energy input using the sine input as compared to a periodic chirp input. Beyond about 11 kHz, the IDE patch actuator driven at 1000 V cannot drive the panel with high enough actuation to make the signal-to-noise ratio high enough for localization and detection of damage in the honeycomb curved panel. Another factor in this experiment is that the damage (added mass that can be removed) is on the interior of the sandwich panel.

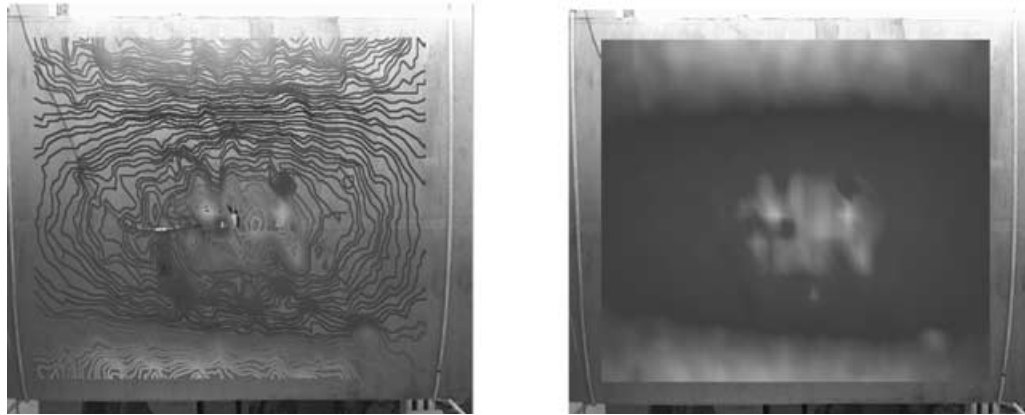


Figure 18. Panel VDS isoclines and contours at 217.2 Hz due to periodic chirp excitation.

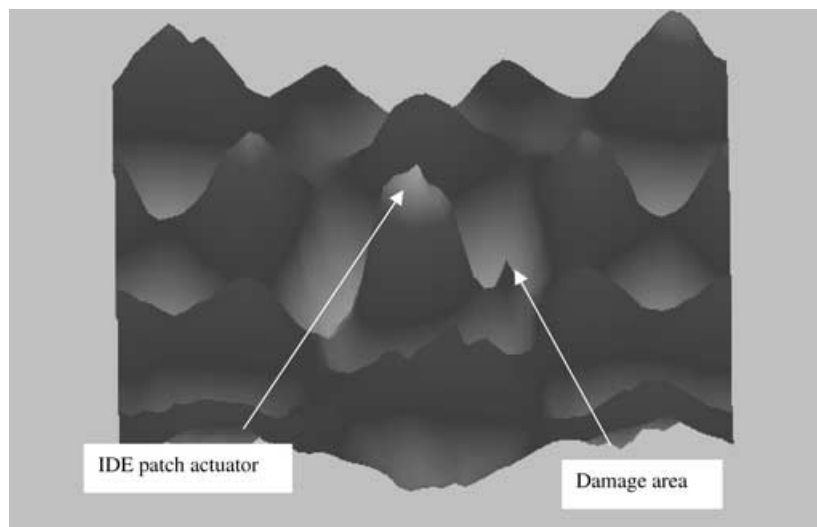


Figure 19. 3-D VDS due to sine excitation at 2.781 kHz.

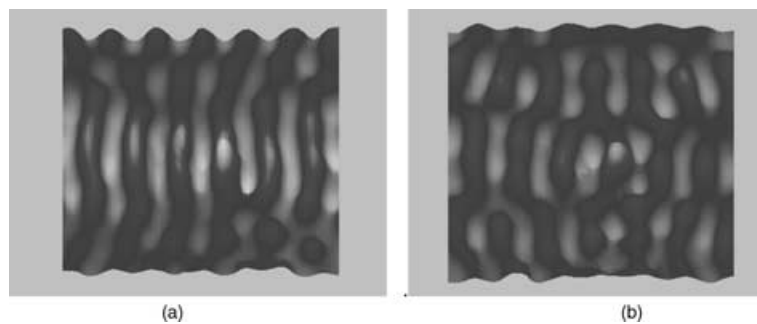


Figure 20. (a) VDS of the panel at 5.122 kHz due to periodic chirp excitation; (b) VDS of the panel due to sine actuation at 5.341 kHz.

This damage may be more apparent at lower frequencies because the actuator does not have enough power to excite the mass on the interior surface at high frequency. Actual damages that would cause a localized stiffness reduction in the core or outer ply may be easier to excite and detect with the high frequency vibration.

Figure 21 shows the PZT IDE patch failing after 3 months of continuous experimentation and actuation at 1000 V. Note how the top Kapton film covering the

electrode peeled off from the PZT wafer and the lower film. This testing apparently shows that the PZT IDE patch may fail after a certain period of actuation. The IDE patch is a preliminary design. A postfailure analysis may be performed to try to improve the reliability of the patch.

In summarizing the panel testing, experimentation showed that the sandwich structure is very stiff and highly damped, and attenuates high frequency waves. It

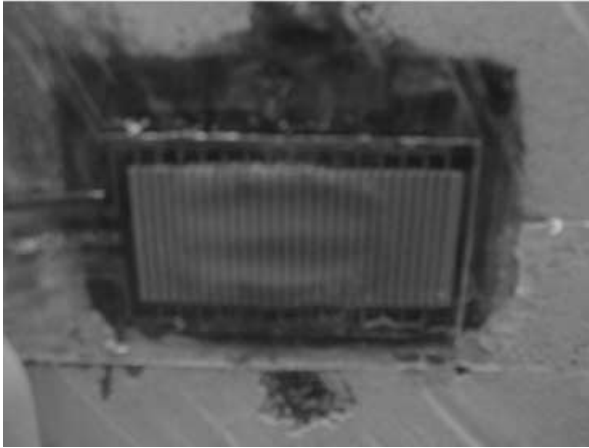


Figure 21. PZT IDE patch failure after a long period of actuation at 1000V continuously. The top Kapton film covering the electrode peeled off from the PZT wafer.

was possible to detect small-simulated damage in the vicinity of the actuator. Therefore, a movable actuator or multiple PZT actuators are necessary for detecting damage on a large structure. In the experiments performed, a mass was bonded to the inside of the sandwich panel and waves were generated using a PZT patch on the outer surface, which was scanned by the laser vibrometer (SLDV). The wave amplitude was reduced at the mass. It is shown that this method can detect damage to the panel, and this method can be used to possibly detect voids at the inner surface of solid propellant tanks.

CONCLUDING REMARKS

The VDS method had been successfully used with different types of structures to detect and localize hidden damages, in this case mainly delamination. The following are the detailed inferences made from the experimental investigations.

(a) From the VDS obtained from the experimental analysis of Carbon Cyanate Composites with seeded delamination:

- It is considerably easier to locate small delamination by using high frequency VDS.
- For low frequency VDS, the relative position of the actuator and the damage in terms of surface distance and ply level distance, and the size of the delamination, can be determining factors for detection and planar localization of the delamination.
- Frequency shift information coupled with VDS can perform surface planar localization of the delaminated zone and also can identify where the delamination is located relative to the midplane.

- Frequency shift correlates with change in moment of inertia suggesting a possible elastic model of the phenomenon.
 - Twisting VDS can be used for damage localization at lower frequencies and appear to be more sensitive to damage than bending modes.
 - VDS can also be used to monitor the integrity of the actuator.
 - The experimental models are validated with FEM model solutions for the specimens.
- (b) VDS can be an effective tool for detection and surface planar localization of internal cracks in large structures as shown in results obtained from the scanning of the curved woven fiberglass panel.
- (c) Conclusions from the experimental analysis of Honeycomb intertank panel using VDS method are:

- Commonly available PZT actuators and amplifiers are not very suitable for actuation for such a highly damped honeycomb panel for successful global detection of damage.
- The new instrumentation tested including the IDE patch actuator QP10Ni, which is capable of actuating up to 1200 V and the high frequency amplifier with a gain of 200 V/V (max voltage is 2 kV) is useful for detection of damage and localization of the damage in the honeycomb structure using the VDS method, without any historical data for the undamaged structure. It is expected that stacked actuators or array of actuators would also provide higher actuation authority needed for detection of internal damages.
- Although the lower frequencies produce higher displacement amplitude, they cannot successfully detect or localize damage because the wavelength of the VDS is too large.
- The natural frequencies in the range of 2.7–10.9 kHz are probably the best range for detection and localization for this type of curved, honeycomb panel and the damage that was simulated by the added mass. There is a limitation at higher frequency (above 11 kHz), the signal-to-noise ratio is lower and ambient noise is more likely to affect the VDS. The actuation energy falls off significantly beyond 11 kHz, even for this instrumentation. This frequency limit could be increased using a smaller PZT patch with a smaller capacitance. Multiple patches could also be used or the patch could be moved to interrogate large structures.
- If the excitation can be produced at a higher frequency, smaller damages will be able to be detected. Potentially, the outline of the honeycomb cells can be shown. This was attempted and is thought to be possible, but not able to be achieved in the current testing.

ACKNOWLEDGMENT

The first author wishes to acknowledge the support and the facilities of the Smart Structures Laboratory at Arizona State University and the NASA-Center for Aerospace Research at North Carolina A&T State University.

REFERENCES

- Chen, S., Venkatappa, S., Petro, S. H., Dajani, J. N. and GangaRao, H.V.S., 1998a. "Damage Detection using Scanning Laser Vibrometer, 3rd International Conference on Vibration Measurements by Laser Techniques," June 16–19, Ancona, Italy.
- Chen, S.E., Petro, S., Venkatappa, S. and GangaRao, H.V.S. 1998b. "Degradation Diagnosis of Structural Members using Strain Energy Approach," *3rd International Conference on Vibration Measurements by Laser Techniques*, June 16–19, Ancona, Italy.
- Cymer ACX, 2001. Quickpack Actuators Manual.
- Doebbling, S.W., Farrar, C.R., Prime, M.B. and Shevitz, D.W. 1996. "Damage Identification and Health Monitoring of Structural and Mechanical Systems from Changes in their Vibration Characteristics: a Literature Review," Los Alamos National Laboratory Report LA-13070-VA5.
- Ghoshal, A., Sundaresan, M. J., Schulz, M. J. and Pai, F. 2000. "Structural Health Monitoring Techniques for Wind Turbine Blades," *Journal of Wind Engineering and Industrial Aerodynamics*, 85(3):309–324.
- Ghoshal, M.J., Sundaresan, M.J. Schulz, and Pai, P.F. 1999. "Damage Detection in Composite Structures using Vibration Measurements," *Sixth International Conference on Composites Engineering*, pp. 245–246, Orlando, FL.
- Kim, H.S., Zhou, X. and Chattopadhyay, A. 2001. "Interlaminar Stress Analysis of Shell Structures with Piezoelectric Patch Including Thermal Loading," *SPIE's 8th International Symposium on Smart Structures and Materials*, Newport Beach, CA. 4326:364–375.
- McHargue, P.L. and Richardson, M.H. 1993. "Operating Deflection Shapes from Time Versus Frequency Domain Measurements," *11th IMAC Conference*, February 1993, Kissimmee, FL.
- Pandey, A.K., Biswas, M. and Samman, M.M. 1991. "Damage Detection from Changes in Curvature Mode Shapes," *J. Sound and Vibration*, 145(2):321–332.
- Richardson, M.H. 1997. "Is it a Mode Shape, or an Operating Deflection Shape," *Sound Vibration Magazine*, 30th Anniversary Issue.
- Schulz, M. J., Ghoshal, A., Sundaresan, M.J., Pai, P.F. and Chung, J.H. 2003. "Theory of Damage Detection Using Constrained Vibration Deflection Shapes," *International Journal for Structural Health Monitoring*, 2(1).
- Schulz, M.J., Naser, A.S., Pai, P.F., Martin, W.N., Turrentine, D. and Wilkerson, C. 1997. "Health Monitoring of Composite Material Structures using a Vibrometry Technique," *4th International Conference on Composites Engineering*, July 6–11, Hawaii.
- Schwarz, B.J. and Richardson, M.H. 1999. "Introduction to Operating Deflecting Shapes," *CSI Reliability Week*, Orlando, FL.
- Sundaresan, M.J., Ghoshal, A., Li, J., Schulz, M.J., Pai, P.F. and Chung, J.H. 2003. "Damage Detection in a Wing Panel Using Vibration Deflection Shapes," *International Journal for Structural Health Monitoring*, (accepted for publication).
- Sundaresan, M.J., Ghoshal, A., Schulz, M.J., Ferguson, F., Pai, P.F. and Chung, J.H. 1999. "Crack Detection using a Scanning Laser Vibrometer," *Second International Conference on Structural Health Monitoring*, September, Stanford University, Stanford, CA.
- Sundaresan, M.J., Ghoshal, A., Schulz, M.J., Ferguson, F., Pai, P.F. and Wilkerson, C. 1999. "Damage Detection using a Laser Vibrometer and Active Fiber Composite Patch," *6th International Conference on Composites Engineering*, June 27–July 3, pp. 735–736, Orlando, FL.
- Sundaresan, M. J., Schulz, M. J., Hill, J., Wheeler, E. A., Ferguson, F., and Pai, P. F., 1999, "Damage Detection on a Wind Turbine Blade Section," *IMAC XVII Conference*, February 8–11, pp. 1359–1365, Orlando, FL.
- Thornburgh, R. and Chattopadhyay, A. 2002. "Modeling the Dynamic Effects of Delamination in Adaptive Composite Laminate," *AIAA 2002-1443, AIAA SDM Conference*, Denver, CO.
- Vold, H., Schwarz, B. and Richardson, M. 2000. "Measuring Operating Deflection Shapes Under Non-stationary Conditions," *IMAC 2000*, San Antonio, TX.
- Waldron, K., Ghoshal, A., Schulz, M.J., Sundaresan, M.J. and Ferguson, F. 2002. "Damage Detection using Finite Element and Laser Operational Deflection Shapes," *J. Finite Elements in Analysis and Design*, 38:193–226.